

Synchronization and Periodic Windows in Globally Coupled Map Lattice

Tokuzo Shimada, Kazuhiro Kubo, Takanobu Moriya
Department of Physics, Meiji University
Higashi-Mita 1-1, Kawasaki, Kanagawa 214, Japan

A globally coupled map lattice (GCML) is an extension of a spin glass model. It consists of a large number of maps with a high nonlinearity and evolves iteratively under averaging interaction via their mean field. It exhibits various interesting phases under the conflict between randomness and coherence. We have found that even in its weak coupling regime, effects of the periodic windows of element maps dominate the dynamics of the system, and the system forms periodic cluster attractors. This may give a clue to the efficient pattern recognition by the brain. We analyze how the effect systematically depends on the distance from the periodic windows in the parameter space.

Key words: synchronization, cluster attractors, periodicity manifestation, globally coupled maps

I. INTRODUCTION

GCML devised by Kaneko [1, 2] is an unfailing source of ideas on the behavior of a complex system composed of many chaotic elements. In its simplest form, it is a model of coupled N logistic maps $f_a(x) = 1 - ax^2$ and evolves in an iteration of a process described by

$$x_i(n+1) = (1 - \varepsilon)f_a(x_i(n)) + \frac{\varepsilon}{N} \sum_{i=1}^N f(x_i(n)) \quad (1)$$

in discrete time n . The nonlinearity of the map f , controlled by a , generally magnifies the variance among the maps, while the averaging interaction, controlled by ε , focuses the maps to the mean field $h(n) = \sum_{i=1}^N f(x_i(n))/N$ and introduce coherence into the maps. Under the conflict between the opposite tendencies the maps exhibit various interesting phases on the a, ε parameter plane [1]. In 90's and early 00's there was important progress concerning the weak coupling regime of the model. Firstly hidden coherence and collective chaos were found [1, 3, 4] in the desynchronized state. Even if the coupling is set to be very weak, maps are not independent random numbers, and consequently the law of large numbers may be violated; there is a long time scale motion which couples the step by step evolution of the maps in a bootstrap. Then, it was found that, even if the coupling is set very weak, the maps systematically synchronize and form various cluster attractors [5, 6] provided that certain tuning condition between the a and ε is satisfied. These were called as periodicity manifestations (PM's) in the turbulent regime and their stability were verified analytically [6]. The most remarkable PM's are the maximally symmetric cluster attractors (MSCA's). Let us denote by p and c the periodicity of the cluster attractor and the number of clusters in the attractor respectively. A period $(p, c = p)$ MSCA is induced by the period p window of the $f_a(x)$ and consists of $c = p$ clusters of maps with almost equal population each other,

which oscillate in period p around the mean field with phases $(\exp(2\pi j/p), j = 0, 1, \dots, p-1)$. Such a MSCA is in general associated by a sequence of cluster attractors; $(p, c = p-1) \rightarrow (p, c = p-2) \rightarrow \dots$, which are produced in order with the increase of the coupling ε . A basic tool to detect the GCML state is the mean square deviation of the mean field $h(n)$ in time defined by

$$\text{MSD} \equiv \frac{1}{T} \sum_{n_1}^{n_1+T} (h(n) - \bar{h})^2, \quad (2)$$

where n_1 denotes appropriate truncation, and \bar{h} is an average of $h(n)$ during n_1 to $n_1 + T$. At MSCA, the symmetry of the population between clusters is high and accordingly the MSD of the mean field $h(n)$ in evolution is very small. On the other hand, the MSD becomes very high due to the lack of one or more clusters in the case of $p, c < p$ cluster attractors. The coexistence of various PM's were reported in AROB [7]. Universality in the formation of such PM's in various coupled maps was clarified in [8].

In this article we present new observations on the formation of PM's in a resurgence of synchronization study of GCML.

To begin with, let us recapitulate how the windows of element maps control the dynamics of GCML. There is a *curve of equivalent (a, ε) points* [6]. That is, if a is increased and ε is *accordingly* increased, GCML should exhibit (qualitatively) the same behavior as before, essentially because the PM's are realized on the balance of randomness and coherence. Then, such curves make altogether a one-parameter family of curves on the (a, ε) plane as depicted in Fig. 1. To derive these curves let us consider one of the MSCA's with period p . In MSCA the mean field is kept constant (say h^*) for its stability; then all maps obey the same time-independent map

$$x_i(n+1) = (1 - \varepsilon)(1 - ax_i^2(n)) + \varepsilon h^*, \quad i = 1, \dots, N. \quad (3)$$

This can be transformed by a scale transformation [9]

$$y_i(n) = \frac{1}{1 - \varepsilon + \varepsilon h^*} x_i(n) \quad (4)$$

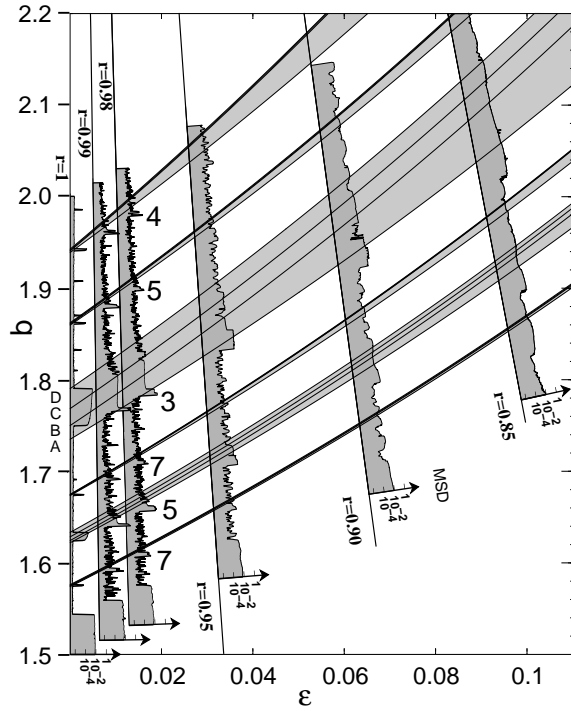


FIG. 1: Foliation of windows $p = 7, 5, 7, 3, 5, 4$ (shaded bands). A, B, C, D indicate respectively the intermittency starting, the opening, the 1st bifurcation (in a window), and the closing point of $p = 3$ window. Pannels show MSD curves at constant r . ($N = 10^6$). Bottom (MSD= 10^7) is aligned with fixed r curve (fitted by a line). Window's effects (PM's) diminish with decreasing r .

into a canonical form

$$y_i(n+1) = 1 - by_i^2(n), \quad i = 1, \dots, N. \quad (5)$$

Here we find that the nonlinearity of the map is reduced by a factor

$$r \equiv \frac{b}{a} = (1 - \varepsilon)(1 - \varepsilon + \varepsilon h^*) \approx 1 - 2\varepsilon, \quad (6)$$

and the value of $b = ra$ must be within the range of the period p window of the map (5); x_i 's in the MSCA oscillate in period p , so y_i 's must also oscillate in period p . Now, let's denote by $y^*(b)$ the long time average of the map (5). Then, from (4), it follows that

$$y^*(b) = \frac{1}{1 - \varepsilon + \varepsilon h^*} h^*. \quad (7)$$

Eliminating h^* from (6) and (7), we obtain

$$a = b/r \quad (8)$$

$$\varepsilon = 1 - \frac{ry^*(b)}{2} - \sqrt{r(1 - y^*(b)) + \left(\frac{ry^*(b)}{2}\right)^2}$$

This determines on the (a, ε) plane a one-parameter (b) family of curves along which the period p MSCA may be formed. These are curves of foliation of periodic windows

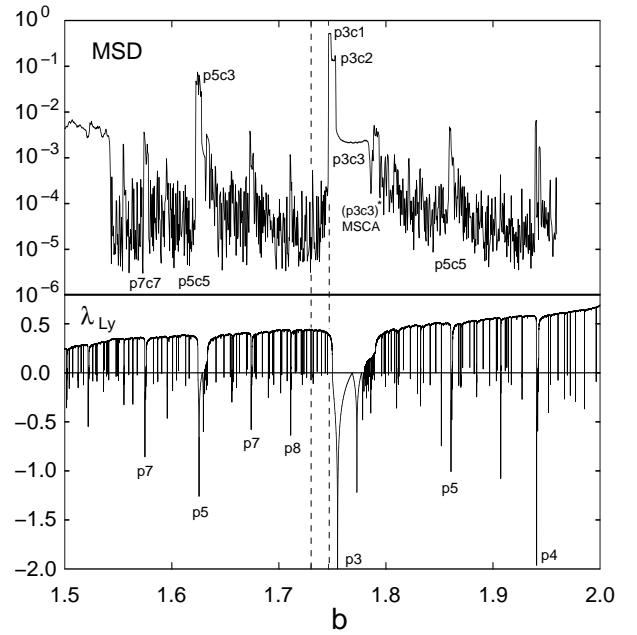


FIG. 2: The MSD of the mean field for GCML at $r = 0.98$ (upper) and the maximum Lyapunov number λ_{Ly} of a single logistic map (lower), both as functions of b . The correspondence between the dominant periodic windows and their MSD valley-peak structures induced by the MSCA and $c = p - 1, p - 2$, clusters is clearly seen.

[6]. In Fig. 1 we observe that near $r = 1$ the MSD curves sensibly reflect the window dynamics of the element maps of GCML and with the decrease of r from one (the larger reduction of non-linearity from a to b), the valley-peak structure of MSD curve diminishes. Accordingly, an extensive study reveals that cluster attractors are formed roughly for $r \geq r_{th}$ and there occur only remnants for $r < r_{th}$ with $r_{th} \approx 0.95$. (We note that the synchronization in the predominant $p3$ window continues to the lower r compared with the other narrower windows.)

In Fig. 2 we compare the MSD curve (sampled at $r = 0.98$) of the GCML with the maximum Lyapunov number λ_{max} of the element map. We find that the MSD curve of the mean field $h(n)$ of GCML is a sensitive mirror of the window dynamics of element maps. In [6] it is pointed out that the MSD curve as a function of ε at fixed a have many valleys and peaks at the smaller ε than for $p3$ foliation, while only few at the larger ε . This anomaly is conjectured as the effect of the difference in the reduction factor r . Present Figures 1 and 2 verify beautifully this conjecture. Below we present our new observations in order.

II. FREE GAS LIMIT AND ADVENT OF CLUSTERS

In Fig. 3 we show how the predominant period three PM's appear in GCML with the decrease of r from one (the increase of ε from zero). The system size is taken as

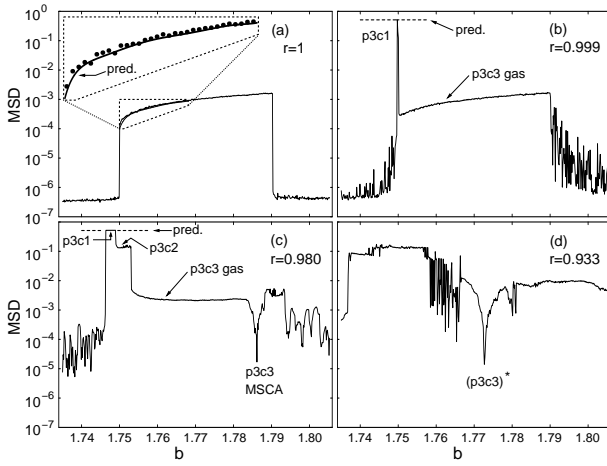


FIG. 3: Variation of the MSD curves with the decrease of r . ($r = 1, 0.999, 0.98, 0.933$.) The inset compares prediction with the measured MSD points (decimated by $1/4$ for comparison).

$N = 10^6$ in order to remove noises. In (a) the MSD curve at $r = 1$ is depicted, which corresponds to an ensemble of free N logistic maps. Let's call this as free gas limit of GCML. Even though there is no interaction, the MSD curve already exhibits an interesting structure. Why the mean field of N independent maps at the large N fluctuates in time? This comes from the basin set structure. The GCML evolves from randomly chosen initial numbers for maps. After certain transient steps all the maps come (independently) into period three attractor. (Precisely, for $b = 1.75 - 1.7685$ the attractor is purely period three, then it repeats period bifurcation to chaos within the window.) Let's denote θ_i ($i = A, B, C$) the population fraction of the maps subject to each of the three bands (with the center value x_A, x_B, x_C) at some time n_0 after the transient. Then, the mean field evolves as

$$\begin{aligned} h(n_0) &= \theta_A x_A + \theta_B x_B + \theta_C x_C \\ h(n_0 + 1) &= \theta_A x_B + \theta_B x_C + \theta_C x_A \\ h(n_0 + 2) &= \theta_A x_C + \theta_B x_A + \theta_C x_B \end{aligned}$$

which is clearly not a constant in time; it oscillates in period three with the MSD dictated by the basin structure characterized by the θ 's and the period three orbits x 's of the single logistic map. We can make a prediction for MSD from the above formula for $h(n)$ (with the variation of the θ 's taking into account) and the analytic orbits x_A, x_B, x_C (for b below the first bifurcation in the $p3$ window). It remarkably explains the measured MSD structure of the free gas GCML as exhibited in the inset.

Then, in (b), at $r = 0.999$, we find that remarkably high MSD peak around the threshold of the $p3$ window. The $p3c1$ cluster attractor is now formed. For other b values, the model is still approximately the free gas $p3c3$ state (with population unbalance).

In (c), at $r = 0.98$, we find now all of the PM's. See Fig. 4 for an enlarged plot. The $p3c1$, and $p3c2$ cluster attractors form in the MSD curve the highest and the sec-

ond high steps respectively. Their evolution is depicted in the respective insets. Then, at higher b , MSD curve shows unbalanced $p3c3$ plateau. Remarkably, around the closing point of the $p3$ window, the MSD valley due to approximate $p3c3$ MSCA is formed. The averaging interaction with $\varepsilon \approx 0.01$ now starts changing the free gas (unbalanced) $p3c3$ into maximally symmetric $p3c3$ cluster attractor ($p3c3$ MSCA).

In (d), at $r = 0.933$, we find $p3c2$ high MSD plateau in the smaller b and a remarkable MSD valley in the middle of the window. The latter is induced by the bifurcated $p3c3$ (that is $p6c6$) as discussed in ref. [6] with analytic consideration on its stability. It is formed around the super-stable point of the $p6$ orbit of the element maps. At this r the GCML dynamics has completely changed from free gas to the synchronization dynamics.

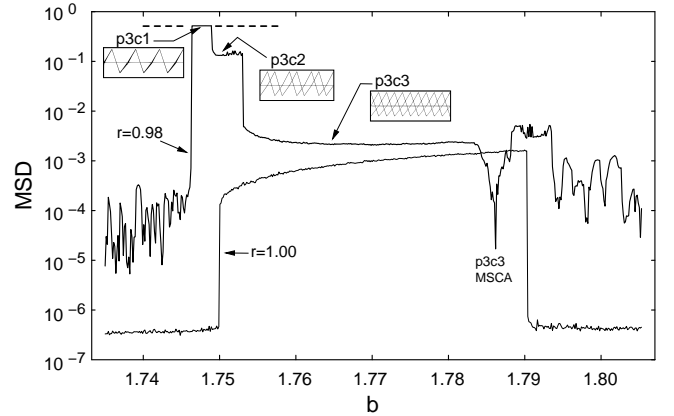


FIG. 4: Change of GCML synchronization with nonlinear parameter b of element maps as seen by the steps of MSD. ($r = 0.98, N = 10^6$.) Insets exhibit corresponding cluster attractor. The seagull structure of MSD curve is induced by $p3c3$ cluster in MSCA configuration. Dashed line is prediction for MSD at $p3c1$ cluster attractor.

III. MECHANISM OF CLUSTERING

Here we clarify the mechanism how the $p3c2$ cluster attractor is realized. It consists of only with two clusters, each in period three motion; a deformed state of $p3c3$ MSCA with a lack of one cluster at the higher coupling. To understand further we adopt a line of argument presented by Shibata and Kaneko to explain the collective motion in GCML [3]. At the $p3c2$ cluster attractor, the mean field oscillate in period three (say, $h_A \rightarrow h_B \rightarrow h_C \rightarrow h_A \rightarrow \dots$). Then, the maps evolve at every three steps by $F_3(x) = F_C(F_B(F_A(x)))$ where

$$\begin{aligned} F_A(x_i) &= (1 - \varepsilon)f_a(x_i) + h_A \\ F_B(x_i) &= (1 - \varepsilon)f_a(x_i) + h_B \\ F_C(x_i) &= (1 - \varepsilon)f_a(x_i) + h_C. \end{aligned}$$

An important observation is that at each step *all* maps obey the *common* logistic map F 's. Therefore it suffice

to study $F_3(x)$ to investigate $p3c2$ cluster attractor. In Fig. 5, $F_3(x)$ with measured values of h_A, h_B, h_C at $p3c2$ cluster attractor are shown along with the line $y = x$. We clearly observe that the case resembles the tangent bifurcation of a single logistic map, but there is an important difference. Now, we observe that only two crossings are stable and each of them attract maps forming two clusters. This is the mechanism for the realization of $p3c2$ cluster attractor. More analytic treatment involving the prediction of the values of h_A, h_B, h_C is under study.

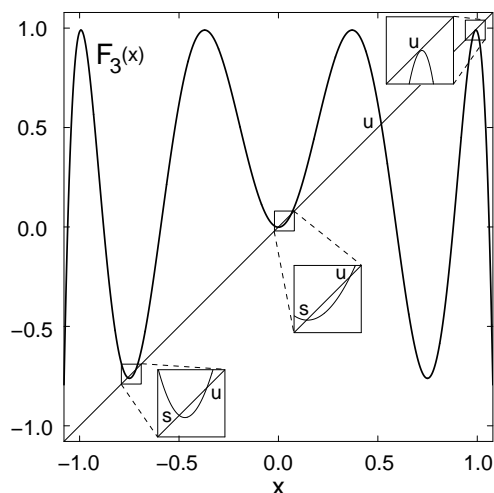


FIG. 5: The mechanism for the $p3p2$ cluster synchronization. $F_3(x) = F_C(F_B(F_A(x)))$ crosses the line $y = x$ at just two stable points, which attract the maps to form eventually two clusters in period 3 motion with $2\pi/3$ mutual phase difference.

IV. MANY SMALL WINDOWS

Up to this point we focused our attention to the predominant period three PM's. Before closing this article we comment on the sharp valleys and peaks in the MSD curve in the lower and upper b regions than the $p3$ window. We show here that they are the reflection of the windows with narrower widths. In fact there is $(2^{p-1} - 1)/p$ windows with a prime number period p [10, 11] and, with the increase of p , they become more dense in the interval

of the nonlinear parameter b . Accordingly the width of the window rapidly becomes narrower. We find that it is sufficient to include the windows with period less than 20 in order to account for the valley and peaks in the lower b region than the $p3$ window. In Fig. 6, we show the location of windows by the zeros of the supertruck functions. It can be seen that these windows are responsible for the valley and peak of the MSD curve ($N = 10^6$ GCML sampled at $r = 0.98$).

In summary we have reported our new observations on the periodicity manifestations of the homogeneous logistic GCML. A new phenomena induced by the basin structure in the free gas GCML is reported. The change of the GCML dynamics from the free gas model to the synchronization with the decrease of r from 1 (the increase of ε from zero) is studied in detail. The mechanism realizing $p3c2$ cluster attractor is shown. The relation between the many small valley-peak structure and the periodic windows are exhibited by the supertruck technique.

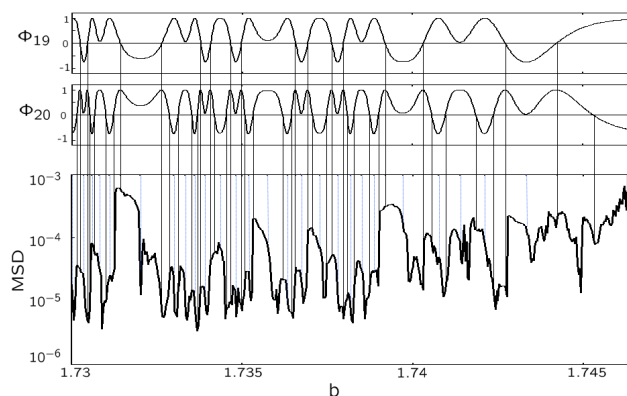


FIG. 6: Valley-peak structure of the MSD curve (lower) and zeros of supertruck curves (upper). Zeros of $p = 19, 20$ windows are shown by solid lines and those with lower period by dotted lines. ($p = 11, 13, 14, 15, 16, 17, 18, 19, 20$ windows contribute respectively 1, 1, 1, 3, 4, 6, 10, 16, 26 zeros for $b \in [1.73, 1.75]$.)

One of us (TS) thanks Kengo Kikuchi for his enthusiasm in the early stage of this work in 1999.

- [1] K. Kaneko, Phys. Rev. Lett. **63**, 219 (1989).
- [2] K. Kaneko, Phys. Rev. Lett. **65**, 1391 (1990).
- [3] T. Shibata and K. Kaneko, Physica **D124**, 177 (1998).
- [4] T. Shibata and K. Kaneko, Phys. Rev. Lett. **81**, 4116 (1998).
- [5] A. P. Parravano and M. G. Cosenza, Cluster dynamics in systems with constant mean field coupling, *chaodyn/9808009*.
- [6] T. Shimada and K. Kikuchi, Phys. Rev. **E62**, pp.3489-3503 (2000)
- [7] T. Shimada and K. Kikuchi, Periodic Cluster Attractors and their Stabilities in the Turbulent Globally Coupled

- Map Lattice, in *Proceedings of International Symposium on Artificial Life and Robotics*, **2**, 313-316 (2001);
- [8] T. Shimada and S. Tukada, Physica **D168-169**, pp. 126-135 (2002).
- [9] G. Perez and H. A. Cerdeira, Phys. Rev. **A46**, 7492 (1992).
- [10] N. Metropolis, M. L. Stein and P. R. Stein, J. Comb. Theory, **A15**, 25 (1973).
- [11] K. Kikuchi and T. Shimada, Transaction of JSCES, paper no. 20020005.